Monthly Report on MSS-1A Magnetic Data Quality for August 2026

Report Author:	Report Approval:
Jiaxuan Zhang	Ligang Li
Jiaxuan ZHANG	Ligang LI
1/Oct/2026	1/Oct/2026

© MISTA. Proprietary and intellectual rights of Macau Institute of Space Technology and Application (MISTA) are involved in the subject-matter of this material and all manufacturing, reproduction, use, disclosure, and sales rights pertaining to such subject-matter are expressly reserved. This material is submitted for a specific purpose as agreed in writing, and the recipient by accepting this material agrees that this material will not be used, copied, or reproduced in whole or in part nor its contents (or any part thereof) revealed in any manner or to any third party, except own staff, to meet the purpose for which it was submitted and subject to the terms of the written agreement.

Table of Contents

1 Introduction 1

1.1 About This Report 1

1.2 Processor Evolution and Instrument Status 1

1.3 Reference 2

2 Event and Anomaly 3

2.1 Discrepancy of F between VFM and CDSM Data Files 3

2.2 VFM Temperature Monitoring 3

2.3 Inter-boresight check 4

2.4 Geomagnetic Activity 6

3 Magnetic Products 8

3.1 Out-of-threshold Values 8

3.2 ASM – VFM Anomaly 10

3.3 ASM – VFM Difference Statistics 13

3.4 Magnetic Components Visual Inspection 16

3.5 $\mathbf{B}_{NEC}$ – CHAOS-8.6 Model Residuals 16

4 Summary 19

1 Introduction

1.1 About This Report

This report presents data-quality results based on MSS-1A Level-2 products reprocessed as Version 07 (V07), applied to observations from August 2026. The assessment covers: (1) detection of data anomalies; (2) evaluation of the vector fluxgate magnetometer (VFM) and the absolute scalar instrument (ASM — the Coupled Dark State Magnetometer, CDSM); and (3) consistency checks between observed and modeled geomagnetic fields.

The scope of this report includes data processing procedures, statistical analysis, and visual inspections of daily magnetic field variations. In addition, when comparing the observed magnetic field (in the NEC frame) with the CHAOS-8.6 internal field model [RD.02], the MMA (Magnetospheric Magnetic field) contribution is included [RD.03]; residuals are examined to provide a quantitative measure of calibration performance and model consistency.

Chapter 1 presents a general overview of the report and its main objectives. Chapter 2 focuses on in-orbit events and anomalies observed during satellite operation, such as changes in instrument temperature ,disturbances and geomagnetic activity (e.g., magnetic storms). Chapter 3 provides a detailed assessment of the magnetic field data quality, including ΔF ($F_{ASM} - |\mathbf{B}_{VFM}|$) time series analysis, residual comparisons with the CHAOS-8.6 model, and visualization of these residuals. Chapter 4 summarizes the overall satellite data status for the month, highlighting any identified anomalies or quality issues.

1.2 Processor Evolution and Instrument Status

The VFM calibration processor was upgraded to version V07 and the entire Level-2 archive was reprocessed (V07) and released in October 2025. For example, an LR file name after the reprocessing looks like:

MSS1A_OPER_VFM_L2_MAG_SCI-LR_20231201T000000_20231201T235959_V0731.cdf

Details of dataset revisions and processor updates are documented in reference [RD.04]. The V07 L2-VFM and CDSM files for observations in August 2026 are the data object of this report and are publicly available from the MSS data portal (https://mss.must.edu.mo/data_download.html). In August 2026, the satellite's magnetic-field instruments were restarted twice. The first restart occurred at around 12:00 UTC on August 7, following timestamp errors in the raw VFM data recorded between August 1 and 7. The timestamps for these seven days were subsequently corrected, and the processed data have been verified to be valid and used for subsequent data production. The second restart was a routine restart carried out at around 16:00 UTC on August 29.

1.3 Reference

[RD.01] Swarm DISC Weekly Report. https://earth.esa.int/eogateway/search?text=&category=Search%20all&instrument=magnetometers,asm,vfm&sortby=NEWEST_FIRST

[RD.02] Kloss, C.; Finlay, C.C.; Olsen, N.; Tøffner-Clausen, L.; Gillet, N.; Grayver, A. (2026) The CHAOS-8 geomagnetic field model, Earth Planets Space, DOI: 10.1186/s40623-025-02352-0.

[RD.03] Swarm Level 2 Processing System - Intermediate validation of Swarm Level 2 Magnetospheric Field Product. https://ftp.space.dtu.dk/data/magnetic-satellites/Swarm/SCARF/CI/Year3/MMA_VALi2C.pdf

[RD.04] MSS-1A VFM and CDSM Data Handbook. https://mss.must.edu.mo/image/handbook/MSS-1A%20VFM%20and%20CDSM%20Data%20Handbook-20251003.pdf

2 Event and Anomaly

2.1 Discrepancy of F between VFM and CDSM Data Files

In the published VFM and CDSM products, both files contain a scalar F. We denote the scalar from the CDSM file as F_{CDSM}, and the scalar from the VFM file as F_{VFM}. We define $\delta F = F_{CDSM} - F_{VFM}$ and report the daily mean, RMS, and maximum of δF in Table 2-1.

Table 2-1: Discrepancy of scalar F between published VFM and CDSM data files in August 2026

Date	Count	Mean	Max
20260807	476	5.14706e-05	0.00011
20260808	13619	26493.2	573753

"Count" indicates the number of data points that exceeded the discrepancy threshold on that day; "Mean δF" represents the average difference in magnetic field magnitude; and "Max δF" denotes the maximum discrepancy detected. Here, Max and Mean are in nT.

We recommend users utilize the F variable from the VFM data files as the scalar measurement value of the MSS-1A satellite, rather than that from the CDSM data files, because the former is used in the in-flight calibration.

2.2 VFM Temperature Monitoring

Figure 2-1 shows the temperature variations for CDC, CSC, and EU during August 2026. The temperature variations remained within the normal range for the month. The maximum temperature observed for CDC was 3.56°C, for CSC 0.63°C, and for EU 28.39°C. The average temperatures were 2.39°C for CDC, -0.88°C for CSC, and 27.05°C for EU. The Huber-weighted RMS values were 0.65°C for CDC, 0.86°C for CSC, and 0.52°C for EU. Here we focus on temperature variability because short-term fluctuations can affect magnetometer calibration and instrument performance.

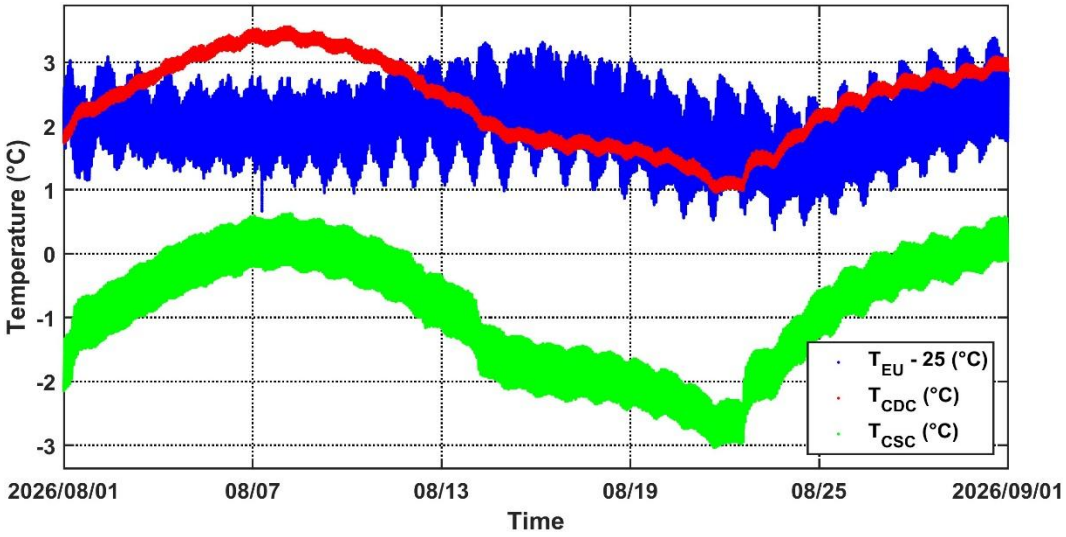


Figure 2-1: Temperature variations of CDC, CSC, and EU during August 2026. The temperature of EU is adjusted by subtracting 25°C.

2.3 Inter-boresight check

The attitude stability of the optical platform from November 2023 to August 2026 is evaluated by monitoring inter-boresight angles (IBAs). Figure 2-2 shows the three camera-pair IBAs (CHUA–CHUB, CHUA–CHUC, CHUB–CHUC, CHU = Camera Head Unit) for the period November 2023 to August 2026. The panels present time series of IBAs after mean removal; the legend of each panel reports the sample mean and the Huber-weighted RMS. Figure 2-3 shows the residual IBAs between the combined quaternion (the L2 VFM product q_NEC_CRF) and the quaternions from individual cameras. These residuals evaluate the improvement in both reliability and accuracy achieved by the combination algorithm relative to single-camera attitude determination. All time series were plotted using 60-s sampling for display clarity.

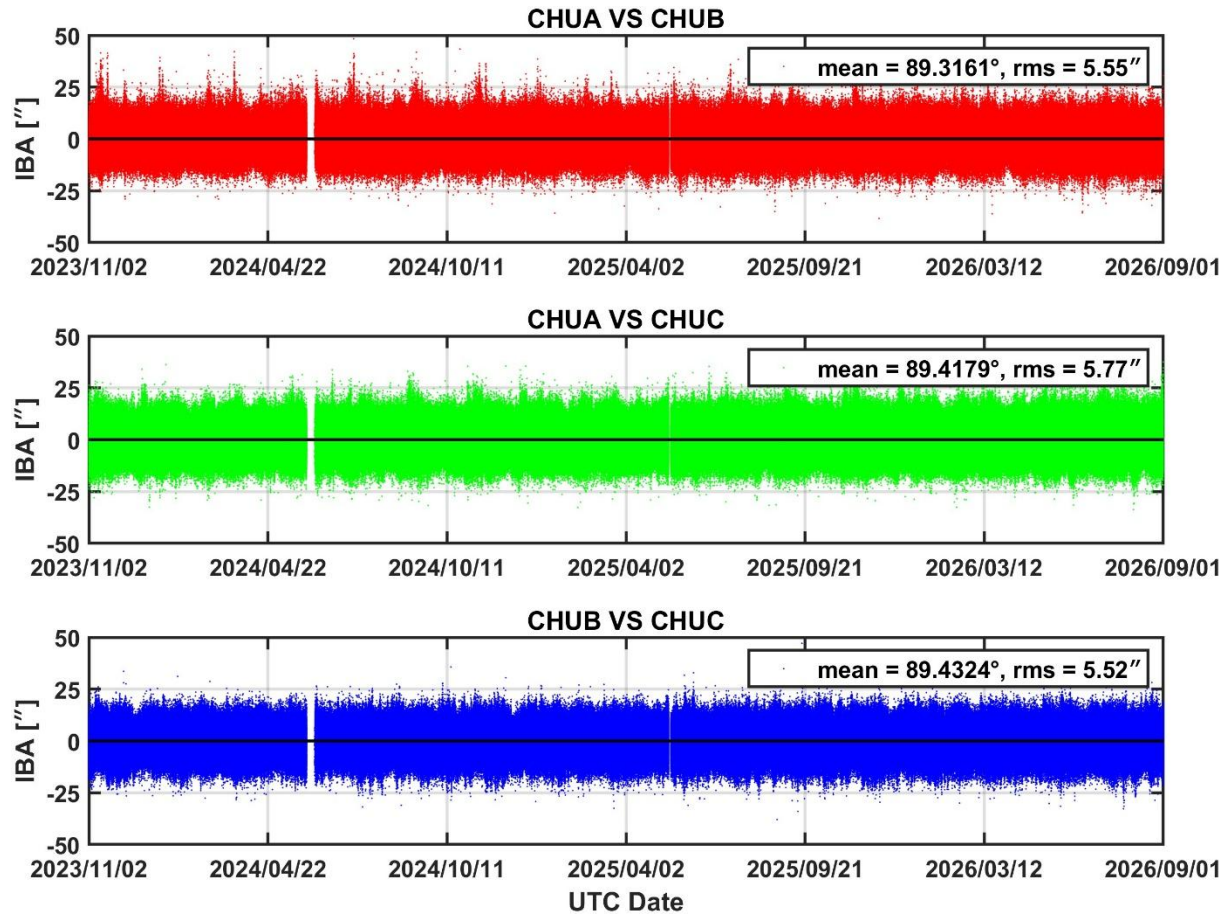


Figure 2-2: Time series of inter-boresight angles (IBA) between the three star-tracker Camera Head Units (CHU): CHUA–CHUB, CHUA–CHUC, and CHUB–CHUC. Values are per-series mean removed and shown in arc-sec. Sampling for plotting: 60 s.

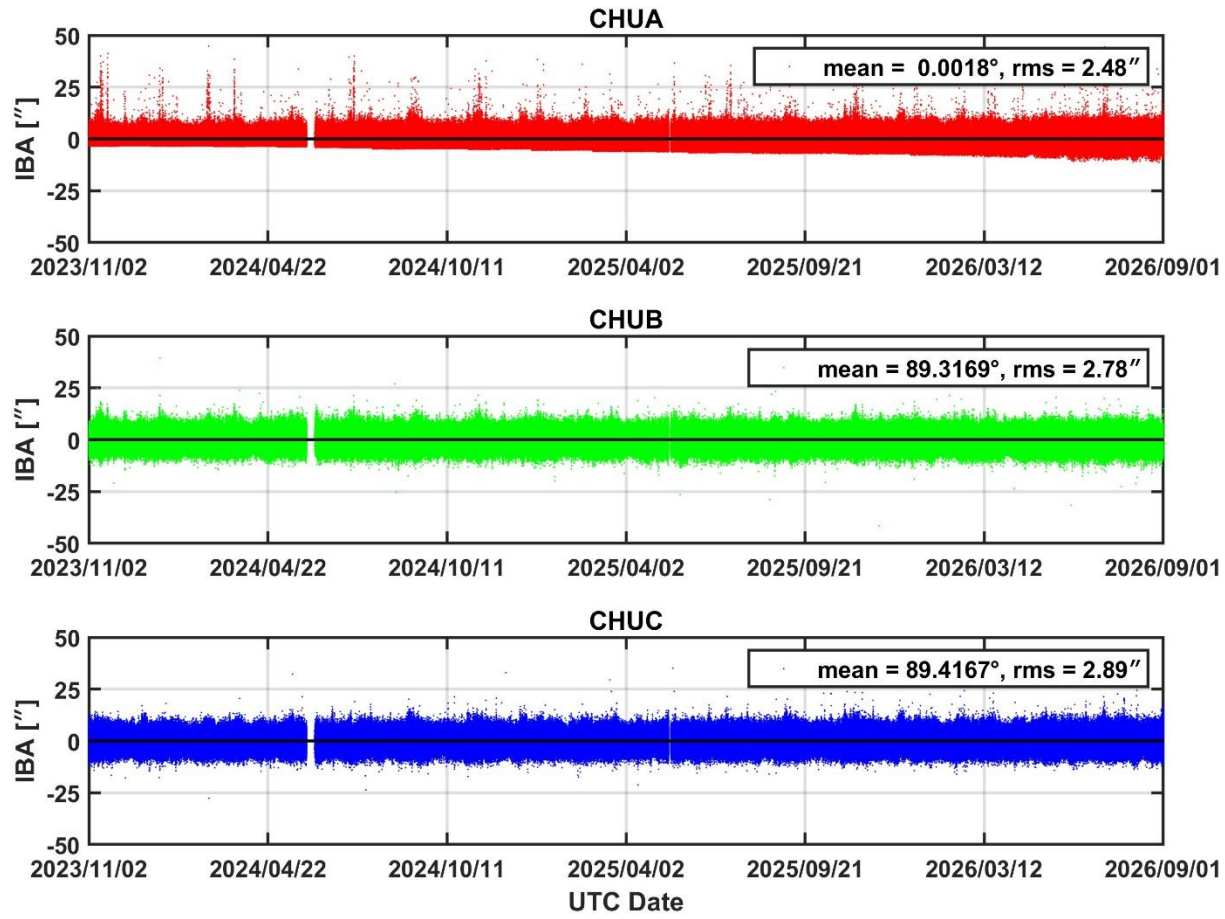


Figure 2-3: Residual IBA time series between the combined quaternion (q_NEC_CRF, L2 VFM) and each single-camera quaternion (units: arc-sec). Small residuals (≲10 arc-sec) indicate good platform stability and effective attitude combination.

Physically, small IBA fluctuations reflect the mechanical/thermal stability of the optical bench and the internal consistency of the quaternion-combination strategy. If residuals between the combined quaternion and the single-camera quaternions remain within ±10 arc-sec, the platform stability and the combination algorithm can be regarded as sufficient for VFM alignment requirements. In our re-analysis for November 2023 to August 2026, the combined-vs-single-camera residuals are largely confined within ± 10 arc-sec, indicating stable platform performance and satisfactory behavior of the attitude-combination method.

2.4 Geomagnetic Activity

Figure 2-4 illustrates the temporal evolution of geomagnetic activity during August 2026, as captured by the Kp index (black line, left axis) and the RC index (blue dashed line, right axis). Several moderate

geomagnetic disturbances were recorded during the month, with Kp values reaching up to 5.7. The RC index reached values as low as -62 nT.

The Kp index can be downloaded from https://kp.gfz-potsdam.de/en/data, and the RC index from http://www.spacecenter.dk/files/magnetic-models/RC/current/.

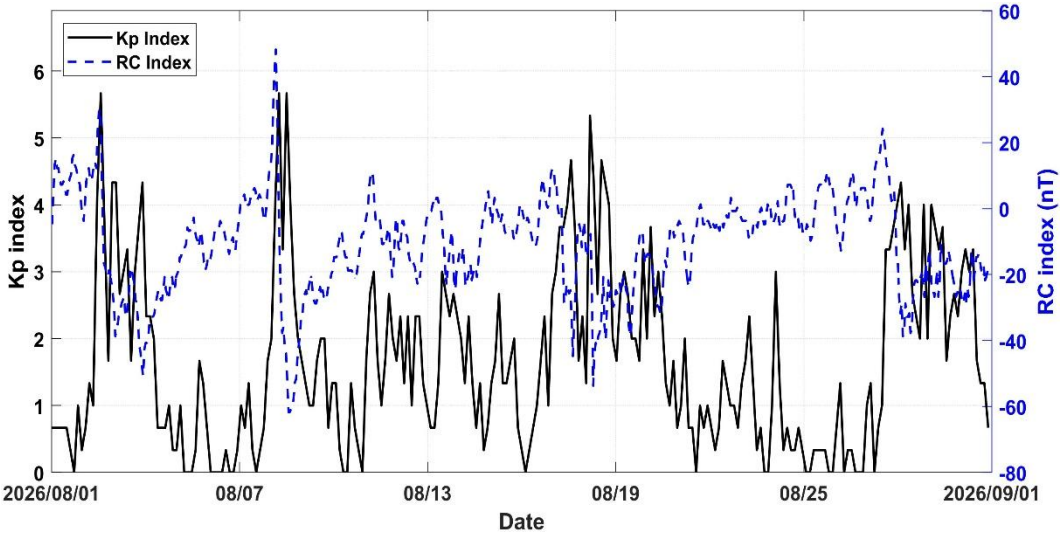


Figure 2-4: Kp (black) and RC (blue) indices showing geomagnetic activity during August 2026.

3 Magnetic Products

This chapter focuses on the quality inspection of the officially released Level 2 scalar (CDSM) and vector (VFM) magnetic field products from the MSS-1A satellite. The analyses aim to assess the temporal stability, detect anomalies, and ensure the reliability of the magnetic measurements. The monitoring includes the following key aspects:

- **Data Range Check:** The magnetic field values of the Level-2 products are systematically checked to ensure they fall within the expected physical range (±18,000 to ±60,000 nT). In addition, the satellite's orbit is verified to remain within the expected spatial coverage (latitude ⩽ 41°, altitude between 415–495 km). To help identify unusual events or anomalous behavior, additional statistics of the Flag_B quality indicator are compiled for further analysis.
- **ΔF Time Series Inspection**: Daily time series of the residuals $\Delta F = F_{ASM} - |\mathbf{B}_{VFM}|$ are visually inspected to monitor the differences between the ASM and VFM. For each day, the mean variation and standard deviation of ΔF are recorded. An alert is raised if the daily mean or RMS of ΔF exceeds ±1 nT. A time series of the RMS of ΔF is then generated.
- **ΔF Statistical Summary**: Mean and standard deviations of ΔF are analyzed over both the current month and the entire available period (since November 2023), providing an overview of the long-term performance of the instruments and highlighting temporal or spatial anomalies.
- **Magnetic Component Inspection**: Daily and monthly variations of the magnetic intensity F and the three $\mathbf{B}_{NEC}$ components are visualized to identify potential jumps, gaps, or systematic errors.
- **Model Residual Analysis**: The observed $\mathbf{B}_{NEC}$ field is compared with the CHAOS-8.6 model, and residual maps are computed and plotted to reveal geophysical signals or potential instrument deviations.

3.1 Out-of-threshold Values

(1) Values exceeding ±60,000 nT or smaller than ±18,000 nT: No out-of-threshold values were detected in the NEC vector components, in the scalar field F derived from CDSM, or in field intensity calculated from $\mathbf{B}_{VFM}$ within the Level-2 data for August 2026.

(2) All recorded values fall within the normal operating bounds:

- |latitude| ⩽ 41°
- 415 km ⩽ height ⩽ 495 km

No positional anomalies were detected this month, indicating nominal satellite orbit and data acquisition.

(3) The Flag_B indicator is used to assess the quality of the magnetic field measurements on board MSS-1A. Each Flag_B value denotes a specific anomaly or condition observed during data acquisition. The flags are defined as follows:

- 0: nominal;
- 1: data is derived through interpolation;
- 2: outliers when $|F_{ASM} - |\mathbf{B}_{VFM}|| > 1$ nT;
- 3: interpolated data points with $|F_{ASM} - |\mathbf{B}_{VFM}|| > 1$ nT;
- 4: position fault when h < 415 km or h > 495 km or abs(latitude) > 41°, where h is satellite height.

For each day in August 2026, the number of observations corresponding to each Flag_B level was counted (expected 86,400 samples/day at 1-Hz); results are summarized in Table 3-1.

Table 3-1: Summary of Flag_B Statistics for August 2026

DATE	num_FlagB_eq0	num_FlagB_eq1	num_FlagB_eq2	num_FlagB_eq3	num_FlagB_eq4
20260801	85795	0	605	0	0
20260802	86246	0	154	0	0
20260803	85996	4	400	0	0
20260804	86144	0	256	0	0
20260805	86281	0	117	2	0
20260806	86354	0	46	0	0
20260807	86250	2	118	30	0
20260808	86056	0	344	0	0
20260809	85607	0	793	0	0
20260810	85318	2	1080	0	0
20260811	85799	2	599	0	0
20260812	85786	0	614	0	0
20260813	85109	0	1291	0	0
20260814	84939	0	1461	0	0
20260815	86261	0	139	0	0
20260816	86193	0	207	0	0
20260817	86060	0	340	0	0
20260818	85577	0	823	0	0
20260819	86120	0	280	0	0

20260820	86316	0	84	0	0
20260821	86373	2	25	0	0
20260822	86338	0	62	0	0
20260823	86351	0	49	0	0
20260824	85789	0	611	0	0
20260825	86369	0	31	0	0
20260826	86176	2	222	0	0
20260827	86305	2	93	0	0
20260828	86339	0	61	0	0
20260829	86149	6	131	114	0
20260830	85927	0	473	0	0
20260831	85678	0	722	0	0

DATE indicates the observation date in the format yyyymmdd. num_FlagB_eq0 represents the total number of records with Flag_B = 0, indicating nominal measurements. Other columns follow the same convention, referring to different Flag_B levels.

3.2 ASM – VFM Anomaly

To validate the physical consistency between vector and scalar magnetic measurements, we define the residual ΔF as the difference between the scalar measurement F_{ASM} and the magnitude of the VFM vector field $|\mathbf{B}_{VFM}|$, such that $\Delta F = F_{ASM} - |\mathbf{B}_{VFM}|$.

It is worth noting that we use δF to denote the difference in the scalar field F between the L2 CDSM file and the L2 VFM file, while ΔF is used to represent the difference between the scalar field F and the vector field strength $|\mathbf{B}|$ in the L2 VFM file.

Under ideal calibration conditions, ΔF should remain close to zero, indicating that the vector magnetometer's sensitivities (scale factors), offsets and non-orthogonalities have been properly corrected. Systematic or large residuals may reflect issues in vector calibration, external disturbances—such as sunlight-induced perturbations, or instrumental failures.

Figure 3-1 shows the temporal evolution of ΔF throughout August 2026 using unscreened VFM and CDSM data, displaying the original range of variation without applying any filtering to the data. Most values fluctuate within ± 1 nT, but occasional spikes appear, indicating short-term disturbances or outliers in the measurements. Overall, the data distribution is centered around zero, suggesting that the instrument calibration is generally stable.

To monitor calibration performance and detect possible anomalies, four key statistics are computed daily throughout the month:

- The minimum and maximum values of ΔF, indicating the range of deviations;
- The mean and root-mean-square (RMS) values of ΔF, quantifying the average daily bias and variability.

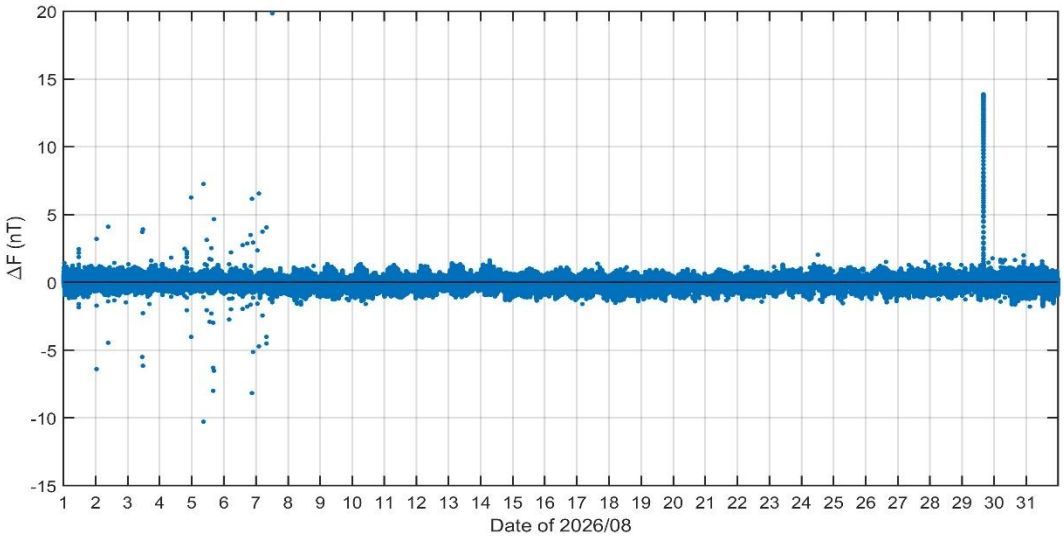


Figure 3-1: Temporal variation of ΔF calculated from unscreened VFM and CDSM data in August 2026.

The table below presents the daily statistical summary of scalar magnetic residuals for August 2026, displaying the daily minimum, maximum, mean, and Huber-weighted RMS values of ΔF. The last row of the table provides a summary of the overall statistics for the entire month. All statistics were computed after applying a uniform data screening, retaining only samples with F and $|\mathbf{B}_{VFM}|$<52,000 nT and |ΔF| ⩽ 20 nT; the same criteria are used throughout the subsequent ΔF analyses.

Table 3-2: Daily statistics of ΔF for August 2026 (Unit: nT)

Date	20260801	20260802	20260803	20260804	20260805	20260806	20260807	20260808
Min	-1.840	-6.413	-6.171	-4.031	-10.293	-8.174	-4.717	-1.646
Max	2.452	4.097	3.909	6.254	7.260	6.172	19.853	1.205
Mean	0.073	0.080	0.084	0.101	0.061	0.030	-0.096	-0.158
RMS	0.333	0.329	0.289	0.239	0.235	0.232	0.268	0.288
Date	**20260809**	**20260810**	**20260811**	**20260812**	**20260813**	**20260814**	**20260815**	**20260816**
Min	-1.340	-1.603	-1.193	-1.113	-1.116	-1.336	-1.347	-1.302
Max	1.362	1.357	1.292	1.238	1.418	1.639	1.023	1.098
Mean	-0.140	-0.133	-0.093	-0.013	0.003	-0.003	-0.121	-0.089
RMS	0.296	0.274	0.289	0.263	0.257	0.285	0.253	0.279
Date	**20260817**	**20260818**	**20260819**	**20260820**	**20260821**	**20260822**	**20260823**	**20260824**
Min	-1.605	-1.517	-1.365	-1.416	-1.338	-1.441	-1.105	-1.450
Max	1.384	1.119	0.915	0.981	0.937	1.140	1.308	2.048

Mean	-0.113	-0.143	-0.090	-0.078	-0.049	-0.033	0.017	-0.026
RMS	0.281	0.272	0.251	0.256	0.282	0.270	0.265	0.280
Date	**20260825**	**20260826**	**20260827**	**20260828**	**20260829**	**20260830**	**20260831**	**202608**
Min	-1.546	-1.475	-1.160	-1.269	-1.326	-1.644	-1.793	-10.293
Max	1.113	1.513	1.501	1.331	13.873	1.982	1.555	19.853
Mean	-0.035	-0.020	-0.010	0.000	0.043	0.063	0.000	-0.036
RMS	0.275	0.266	0.271	0.273	0.296	0.294	0.305	0.287

Violation of ΔF threshold:

- Mean residuals (absolute value>1 nT): no violations.
- RMS residuals (>1 nT): no violations.

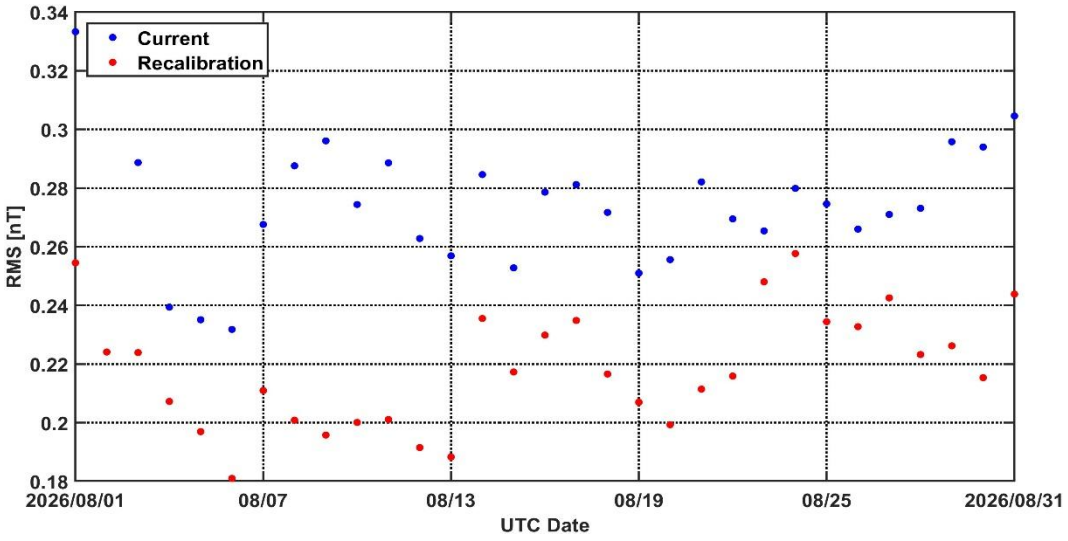


Figure 3-2: ΔF RMS statistics of MSS-1A Level 2 data (blue) and daily in-flight recalibration results (red) for August 2026.

Figure 3-2 presents the Huber-weighted root-mean-square (RMS) of ΔF for MSS-1A Level 2 VFM data in August 2026 (blue dots). The daily in-flight recalibration results (red dots) show reduced RMS values compared with the baseline processing. This improvement is more likely attributable to imperfect original calibration parameters; daily recalibration reduces calibration-related residuals.

For overall data calibration (blue dots), a quality filter was applied to remove physically unreasonable data points. This ensured that outliers would not bias the calibration results. The same screening criteria were also applied in the daily nine-parameter recalibration. In addition, the use of the Huber weighting scheme further improves robustness by down-weighting residuals from outlier points during RMS computation.

Figure 3-3 displays the temporal variation of ΔF RMS values in VFM files since November 2, 2023. Overall, the RMS variation of MSS-1A data remains stable.

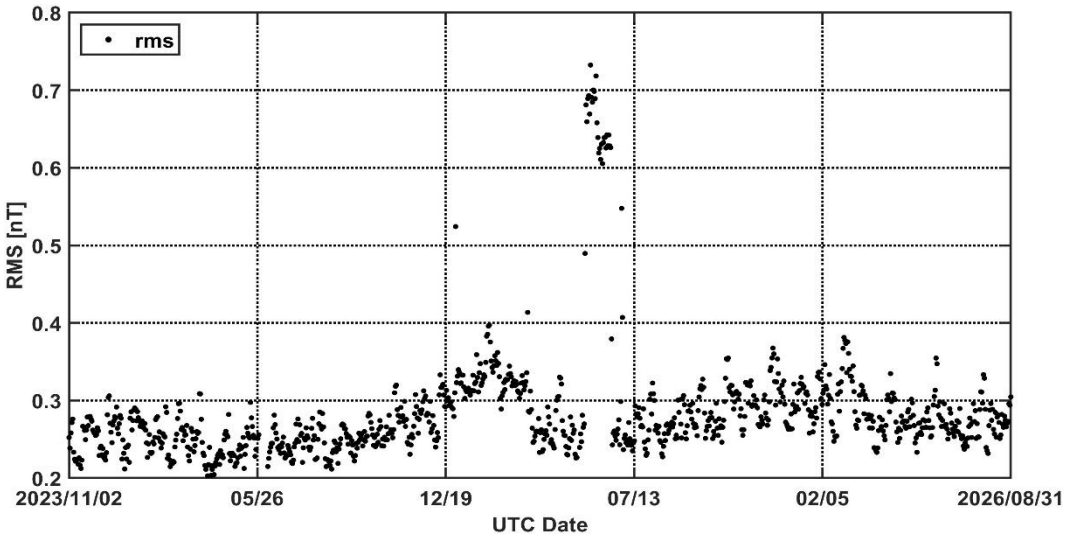


Figure 3-3: Temporal evolution of ΔF RMS values in VFM data from November 2023 to August 2026.

3.3 ASM – VFM Difference Statistics

Figure 3-4 shows the daily mean (circles) and standard deviation (crosses) of ΔF of August 2026. Figure 3-5 extends this analysis by presenting the daily mean and standard deviation values of ΔF from November 2023 to August 2026. The subsequent two plots (Figures 3-6 and 3-7) present ΔF analyses for August 2026. Figure 3-6 shows the time series for the month, with daytime and nighttime measurements represented by red and blue dots, respectively. The residuals primarily remain within ±2 nT, though occasional outliers are present. Statistical metrics displayed in the top-left corner indicate consistent mean and RMS values for both daytime and nighttime ΔF throughout the month. Figure 3-7 illustrates the spatial distribution of ΔF across longitude and latitude coordinates.

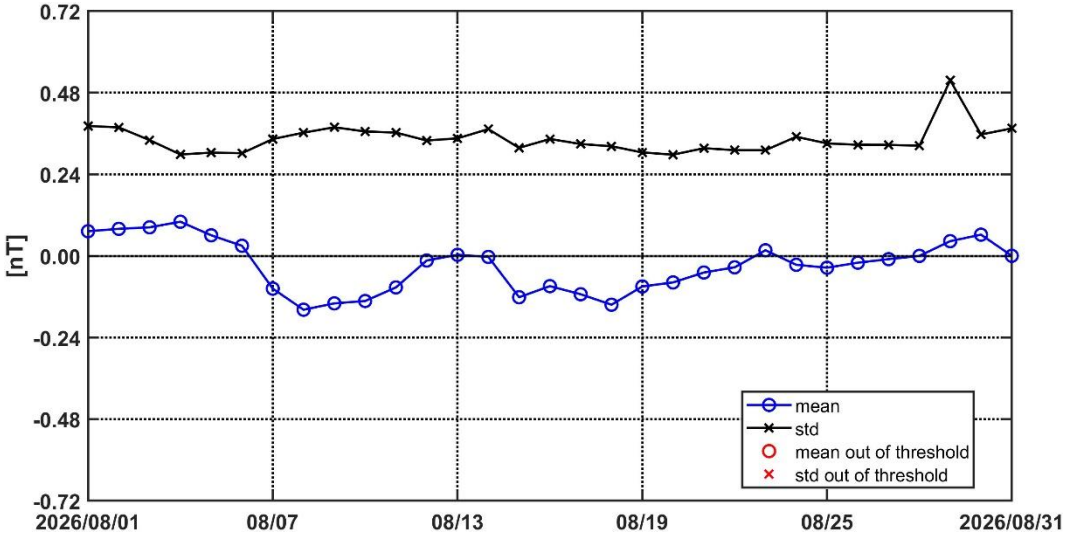


Figure 3-4: Daily mean and standard deviation values of ΔF in August 2026. Red circles and crosses indicate days where the absolute values of the mean and root-mean-square (RMS) residuals exceed 1 nT. (This situation does not occur during this month). The standard deviation shown is computed as the sample standard deviation (divided by n–1).

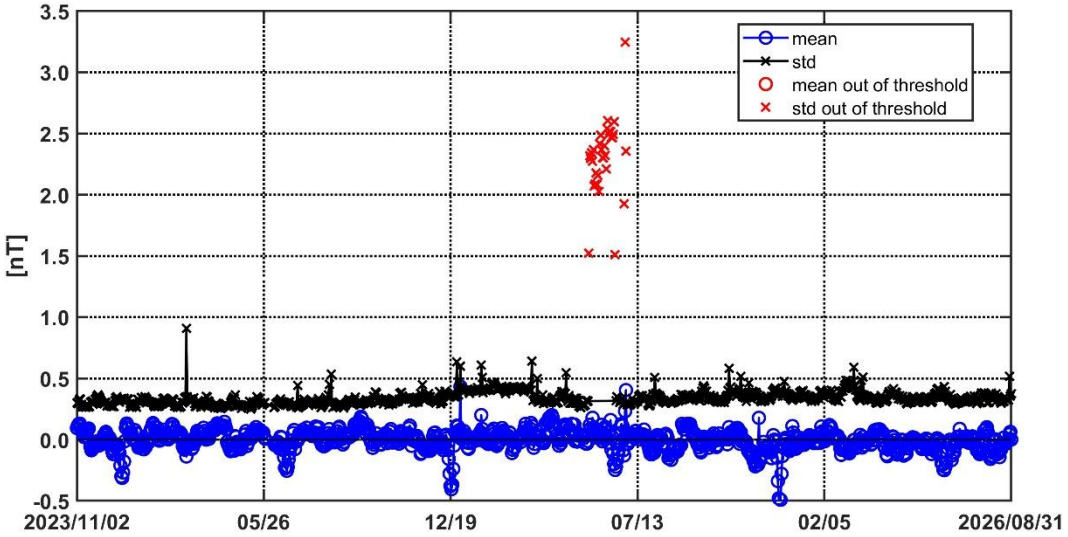


Figure 3-5: Daily mean and standard deviation values of ΔF from November 2023 up to August 2026.

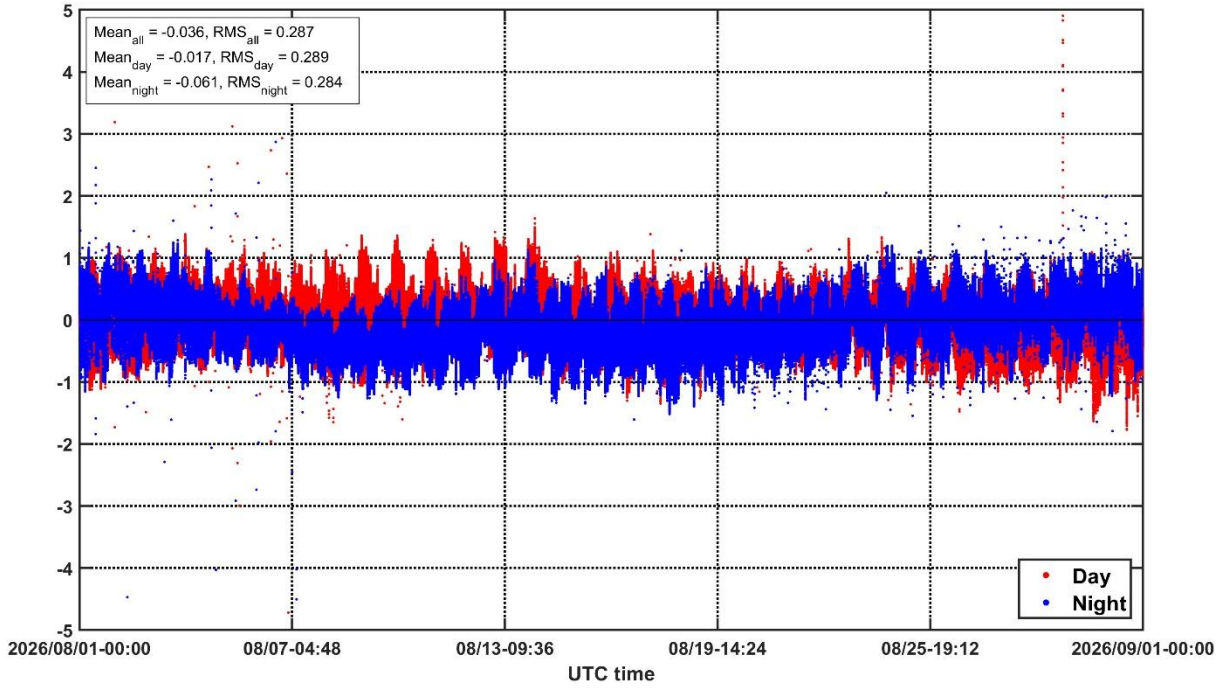


Figure 3-6: ΔF time series during August 2026 (unit: nT). Red and blue dots represent daytime and nighttime measurements, respectively.

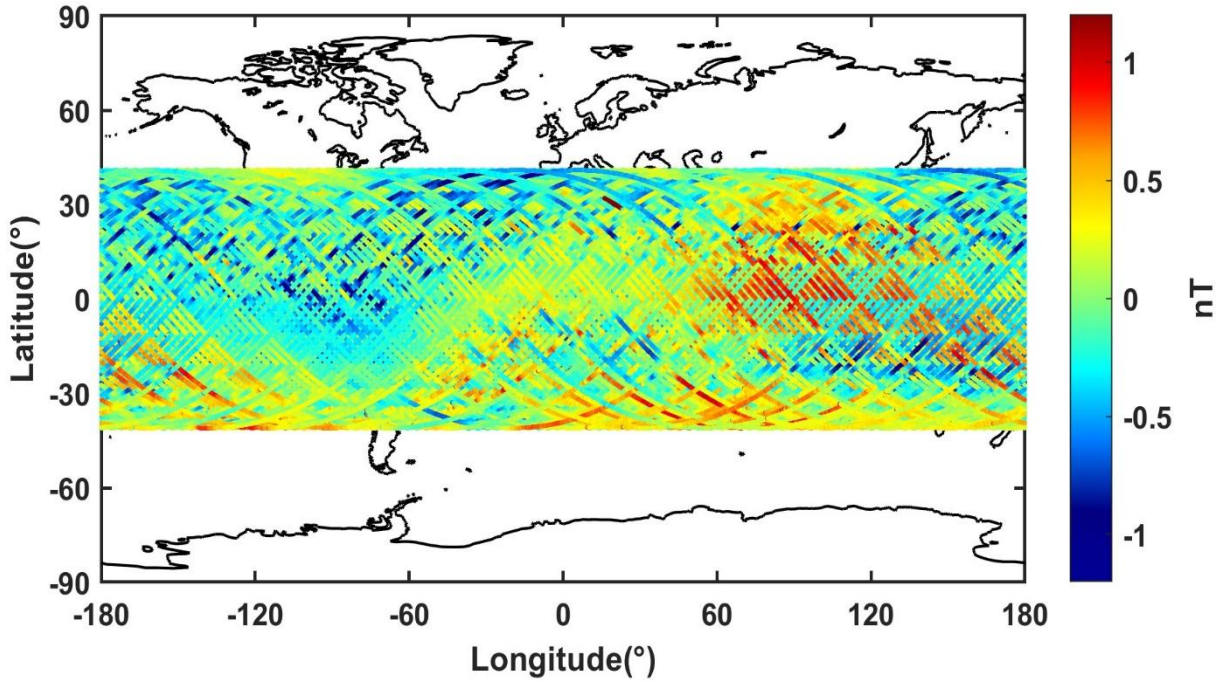


Figure 3-7: Residuals ΔF for August 2026 are plotted on the world map.

3.4 Magnetic Components Visual Inspection

Below are four sub-figures showing global maps of variables F_{ASM} and $\mathbf{B}_{NEC}$ for August 2026. The scalar field F_{ASM} is derived from ASM measurements, and the $\mathbf{B}_{NEC}$ components are obtained from VFM measurements in the NEC frame. Visual inspection confirms that the measured magnetic field is broadly consistent with current geomagnetic model outputs and reveals no large-scale artifacts in the data.

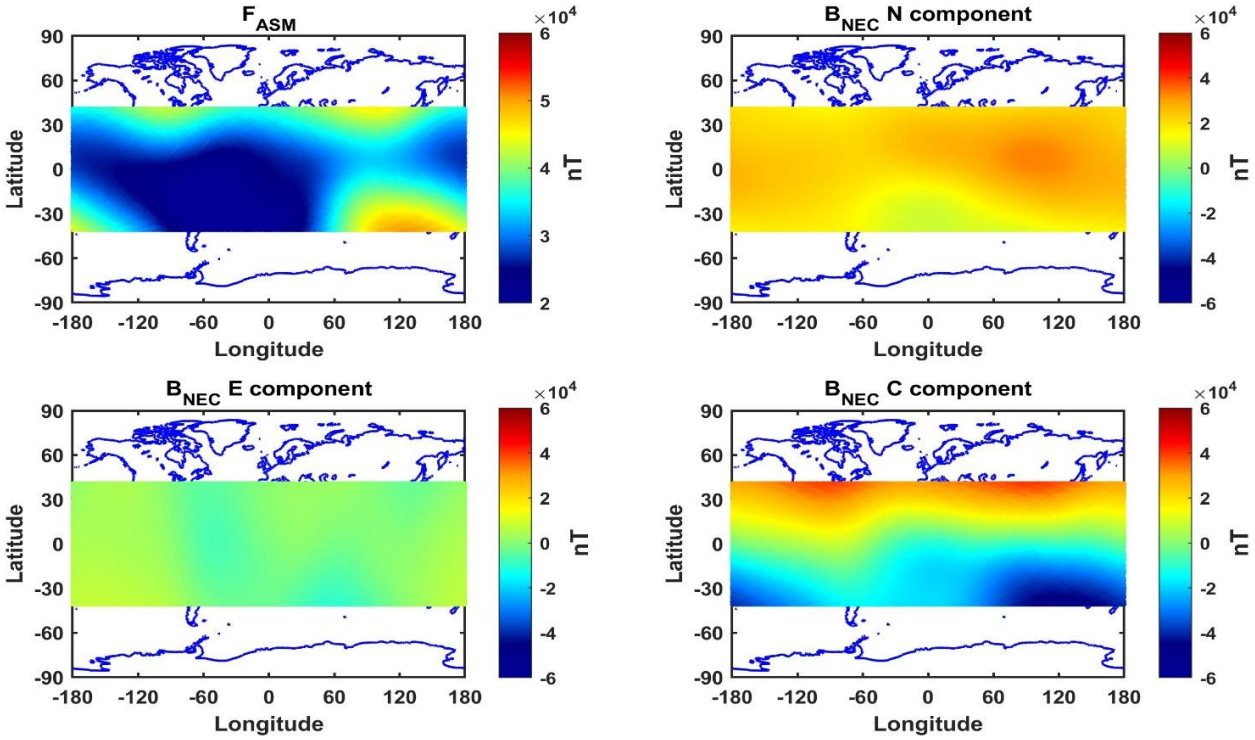


Figure 3-8: World map plots of the geomagnetic field and components for August 2026. From top to bottom: F_{ASM} from ASM measurement, and B_N, B_E, B_C components in the NEC frame from VFM measurement.

3.5 B_{NEC} – CHAOS-8.6 Model Residuals

Figures 3-9 and 3-10 show the differences between MSS-1A magnetic field measurements and the CHAOS-8.6 model in August 2026. The model includes the main (core) field, the lithospheric (crustal) field up to spherical-harmonic degree 60, and magnetospheric (and induced) contributions.

For time intervals where CHAOS does not provide up-to-date external-field (magnetospheric /induced) estimates, we compute those external contributions using the MMA model.

Figure 3-9 displays the residuals $\Delta B = \mathbf{B}_{NEC} - \mathbf{B}_{CHAOS}$ as a function of colatitude, while Figure 3-10 presents the same residuals as a function of UTC time. From top to bottom, the panels show the northward (ΔB_N), eastward (ΔB_E), downward (ΔB_C), and scalar (ΔF_{CHAOS}) residuals. Here and throughout this section, ΔF_{CHAOS} denotes the scalar difference between the measured F_{ASM} and the CHAOS-8.6 model value. In August 2026, the residuals remained generally stable at low and mid latitudes (|latitude| $\leqslant$ 41°), with extreme values reaching -74.62 nT, 103.58 nT, 46.76 nT, and -73.65 nT for ΔB_N, ΔB_E, ΔB_C and ΔF_{CHAOS}, respectively.

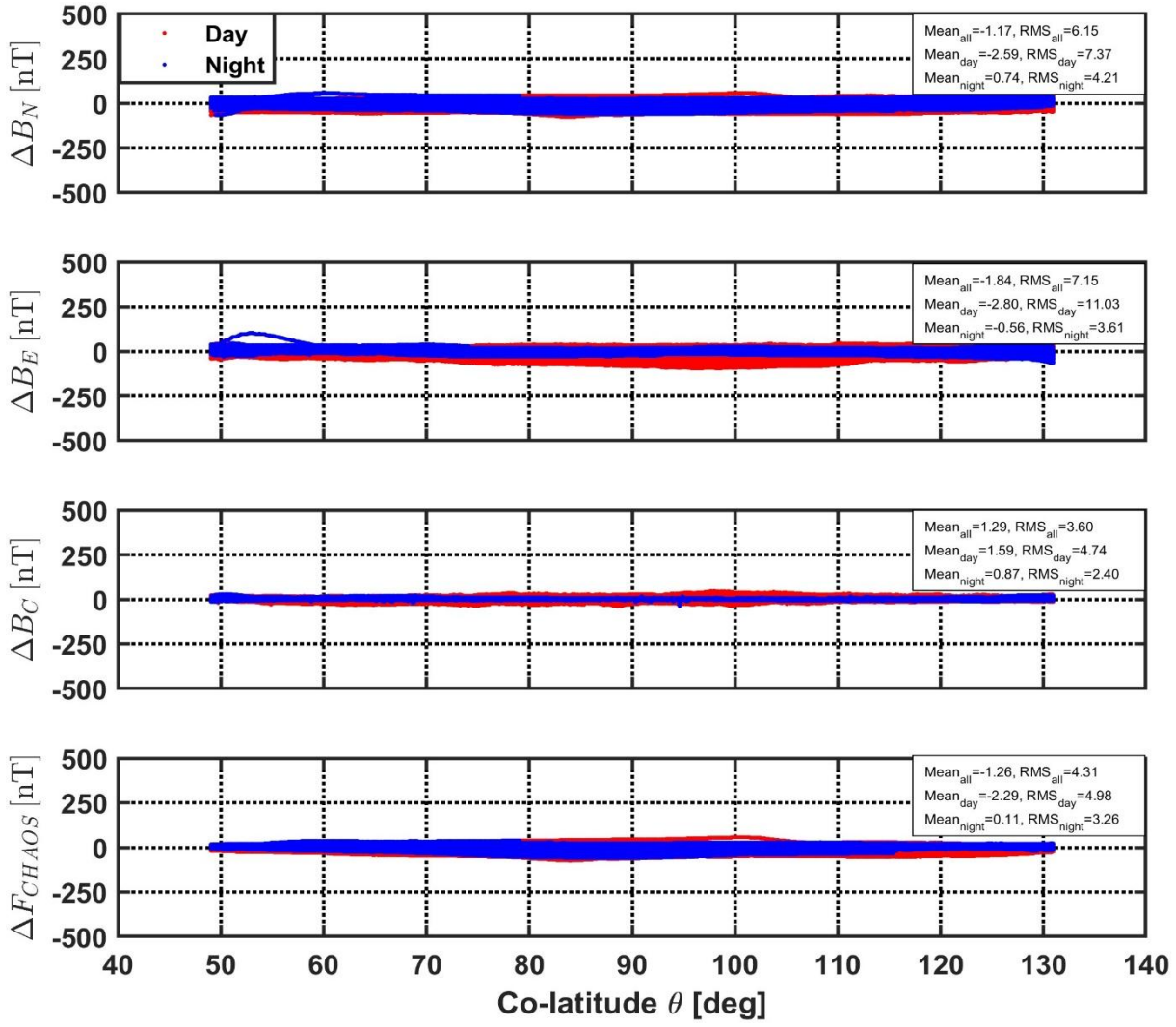


Figure 3-9: Differences between measurements and the CHAOS-8.6 model along the colatitude. From top to bottom: differences of northward, eastward, downward and scalar components.

Figure 3-9 illustrates residual amplitudes that remain stable under predominantly quiet geomagnetic conditions. No significant storm-related enhancements are observed during this month, and similar behavior is evident in Swarm data.

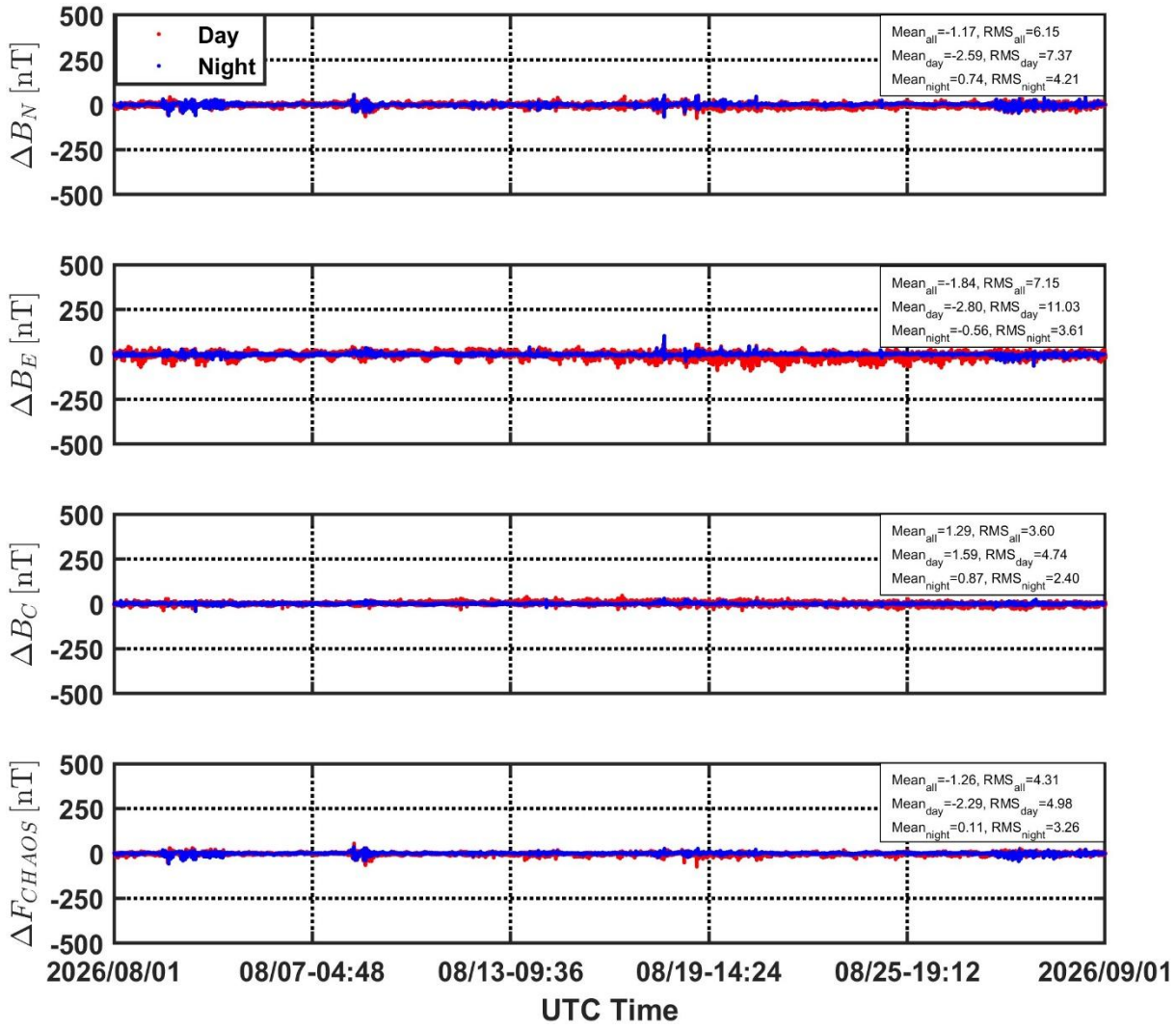


Figure 3-10: Differences between measurements and the CHAOS-8.6 model along the UTC time. From top to bottom: differences of northward, eastward, downward and scalar components.

Figure 3-10 presents the residual time series between the MSS-1 magnetic-field measurements and the CHAOS-8.6 model for August 2026. The residuals exhibit overall stable behavior under predominantly quiet geomagnetic conditions, consistent with Swarm observations at low and mid latitudes.

4 Summary

This report provides a comprehensive assessment of the MSS-1A satellite magnetic field data quality during August 2026. The main findings are as follows:

- **Data Integrity:**
  No physically unrealistic values were found in the $\mathbf{B}_{\mathrm{NEC}}$, $\mathbf{B}_{\mathrm{VFM}}$, or scalar (F) components of the Level-2 data. No out-of-threshold values in VFM products were observed this month. Scalar–vector differences remained consistently within acceptable bounds.

- **Satellite Position Check:**
  Satellite altitude and latitude were checked against thresholds of 415–495 km and |latitude| $\leqslant$ 41°. No positional anomalies were detected in August 2026, and the data can be used with confidence.

- **Instrument Performance:**
  Temperature readings from CDC, CSC, and EU remained stable. The instruments were restarted twice during the month: an unscheduled restart at around 12:00 UTC on August 7 following timestamp errors in the raw VFM data of August 1–7 (subsequently corrected and verified as valid), and a routine restart at around 16:00 UTC on August 29. Instrument recovery was nominal in both cases, with no data loss or degradation in data quality.

- **Calibration and Model Residuals:**
  Overall, daily mean and Huber-weighted RMS values of ΔF were generally within ± 1 nT during August 2026. Daily in-flight recalibration using LR data further reduced ΔF scatter. Comparisons with the CHAOS-8.6 model also confirmed that residuals in the NEC frame were well within expected bounds.

In conclusion, the MSS-1A magnetic field data for August 2026 is complete and of high quality.